The EMBO Journal Vol.16 No.14 pp.4205–4216, 1997

The three-dimensional structure of a T-cell antigen receptor VαVβ heterodimer reveals a novel arrangement of the Vβ domain

Dominique Housset, Gilbert Mazza[1], Claude Grégoire[1], Claudine Piras, Bernard Malissen[1,2] and Juan Carlos Fontecilla-Camps[2]

Laboratoire de Cristallographie et Cristallogénèse des Protéines, Institut de Biologie Structurale 'Jean-Pierre Ebel' CEA-CNRS, 41 avenue des Martyrs, 38027 Grenoble cedex 1 and [1]Centre d'Immunologie INSERM-CNRS de Marseille-Luminy, Case 906, 13288 Marseille cedex 9, France

[2]Corresponding authors
e-mail: bernardm@ciml.univ-mrs.fr or juan@lccp.ibs.fr

D.Housset and G.Mazza contributed equally to this work

The crystal structure of a mouse T-cell antigen receptor (TCR) Fv fragment complexed to the Fab fragment of a specific anti-clonotypic antibody has been determined to 2.6 Å resolution. The polypeptide backbone of the TCR Vα domain is very similar to those of other crystallographically determined Vαs, whereas the Vβ structure is so far unique among TCR Vβ domains in that it displays a switch of the c″ strand from the inner to the outer β-sheet. The β chain variable region of this TCR antigen-binding site is characterized by a rather elongated third complementarity-determining region (CDR3β) that packs tightly against the CDR3 loop of the α chain, without leaving any intervening hydrophobic pocket. Thus, the conformation of the CDR loops with the highest potential diversity distinguishes the structure of this TCR antigen-binding site from those for which crystallographic data are available. On the basis of all these results, we infer that a significant conformational change of the CDR3β loop found in our TCR is required for binding to its cognate peptide–MHC ligand.

Keywords: antigen-binding site/complementarity-determining region/crystal structure/T-cell receptor/Fv fragment

Introduction

The specific recognition of antigen by T cells and its ensuing transduction into intracellular signals are accomplished by a multi-subunit complex denoted as the T-cell receptor (TCR)–CD3 complex. The TCR α and TCR β polypeptides, which confer antigen-binding capacity to these membrane-bound complexes, consist of an amino-terminal variable (V) region and a carboxy-terminal constant (C) region. The determination of the three-dimensional structure of an isolated TCR β chain (Bentley *et al.*, 1995) and of a homodimer of Vα domains (Fields *et al.*, 1995) indicated that both Vα and Vβ regions are structurally related to the V domains of the heavy (H) and light (L) chains of immunoglobulins (Igs), and showed that peptide loops homologous to Ig complementarity-determining regions (CDRs) protrude at the membrane-distal ends of both TCR Vα and Vβ domains where they collectively form the antigen-binding site. As previously observed for Ig V domains, the first and second CDR equivalents are encoded within V gene segments, whereas the third CDR equivalent is formed during somatic DNA recombination events involving the juxtaposition of Vα and Jα gene segments in TCR α chain genes, and of Vβ, Dβ and Jβ gene segments in TCR β chain genes. During V(D)J recombination, the coding ends of the TCR gene segments are subjected to various degrees of base deletion, addition or both. Due to this extensive junctional diversity, the Vα and Vβ CDR3s are responsible for most of the diversity observed in αβ TCRs (Davis and Bjorkman 1988; Jores *et al.*, 1990). The αβ TCRs recognize peptides that are bound to either class I or class II products of the major histocompatibility complex (MHC). X-ray structures of MHC class I molecules complexed with different peptides have shown that the latter are buried in the groove formed between the α1 and α2 helices, leaving only a few of their side chains available for direct TCR contact (Fremont *et al.*, 1992, 1995; Zhang *et al.*, 1992; Madden *et al.*, 1993; Young *et al.*, 1994). These data have led to the view that TCR VαVβ regions most likely recognize a composite surface made of residues belonging to a given antigenic peptide and to both MHC α1 and α2 helices (Sun *et al.*, 1995).

Here we report the 2.6 Å resolution structure of a TCR single chain Fv fragment (scFv) derived from the KB5-C20 mouse cytotoxic T cell clone complexed to a Fab fragment of the specific monoclonal anti-clonotypic antibody Désiré-1 (Albert *et al.*, 1982; Hua *et al.*, 1985; Hue *et al.*, 1990; Grégoire *et al.*, 1991, 1996). While this manuscript was in preparation, two reports on TCR crystal structures have appeared. The first one describes the structure of a complete αβ TCR ectodomain derived from the 2C mouse alloreactive cytotoxic T-cell clone (Garcia *et al.*, 1996a). Interestingly, the antigen-binding sites of the KB5-C20 and 2C TCRs use distinct Vα–Vβ gene segment combinations and exhibit TCR β-chain CDR3 region lengths which lie at opposite tails of the TCR β CDR3 size distribution (Candéias *et al.*, 1991; Pannetier *et al.*, 1993). Despite these marked differences, both TCRs recognize the same MHC class I molecule (H-2K^b) when complexed to different peptides. Comparison of their combining sites thus provides a unique opportunity to examine the range of TCR conformational variability allowed for the recognition of a given class I MHC molecule. The second report corresponds to the structure of a complex containing a human αβ TCR bound to an HLA-A2 molecule loaded with a nonapeptide derived from the HTLV-1 virus (A6 TCR–Tax–HLA-A2 complex, Garboczi *et al.*, 1996). Using the atomic coordinates of

Table I. Data collection statistics

	Resolution (Å)	No. of measurements	No. of reflections [$F>3\sigma(F)$]	R_{sym} (last shell)	Completeness (%) (last shell)	Redundancy (last shell)	$<I/\sigma(I)>$ (last shell)
Form 1	2.9	147 342	29 732 (27 746)	0.091 (0.400)	86.7 (67.4)	5.0 (3.1)	7.2 (1.8)
Form 2	2.6	75 774	24 517 (18 474)	0.086 (0.300)	86.7 (75.6)	3.1 (2.5)	–

Table II. Molecular replacement and refinement statistics

Molecular replacement statistics

	Resolution range (Å)	*R*-factor (%)	Correlation coefficient (%)
One C_κ–C_{H1}	15.0–3.5	58.6	13.9
One V_L–V_H	15.0–3.5	59.0	11.1
Two C_κ–C_{H1}	15.0–3.5	53.4	35.8
TwoV_L–V_H	15.0–3.5	54.1	32.9
Two Fabs	15.0–3.5	51.3	40.7
Two Fabs + two Vα–Vβ	15.0–3.5	48.8	48.3
	10.0–2.9	48.7	48.1

Refinement statistics

Resolution (Å)		No. of reflections	No. of atoms	*R*-factor	R_{free}	Stereochemistry (SD from ideality)	
Form 1	$F>3\sigma(F)$	26 296		24.9	31.6	bonds	0.014 Å
8.0–2.9			10 280			angles	0.039 Å
	all	28 266		27.0	33.9		
Form 2	$F>3\sigma(F)$	18 105		21.0	30.4	bonds	0.013 Å
10.0–2.6			5438			angles	0.034 Å
	all	20 232		22.1	31.5		

$R_{sym} = \sum_{\mathbf{h}} \sum_{i} |I_{i\mathbf{h}} - \langle I \rangle_{\mathbf{h}}| / (\sum_{\mathbf{h}} \sum_{i} \langle I \rangle_{\mathbf{h}})$.

R-factor $= \sum_{\mathbf{h}} |F_{obs} - F_{calc}| / \sum_{\mathbf{h}} |F_{obs}|$, correlation coefficient $= \langle (F_{obs} - \langle F_{obs} \rangle)(F_{calc} - F_{calc} \rangle) \rangle / \langle F_{obs} \rangle \langle F_{calc} \rangle$.

R_{free} is an *R*-factor calculated on a subset of reflections (5%), not used in the refinement.
Non-crystallographic symmetry restraints have been used during refinement of crystal form 1.

this ternary complex, we have carried out rigid-body rotations of the KB5-C20 TCR scFv and H-2K^b structures onto the positions occupied by their respective human counterparts, and found that a significant conformational change of the KB5-C20 CDR3β loop is required for binding to its cognate peptide–MHC ligand. Moreover, this hypothetical model allowed us to define a minimum set of plausible interactions between the KB5-C20 TCR and H-2K^b molecule, and to compare them with the ones reported in the A6 TCR–Tax–HLA-A2 complex.

Results and discussion

Overall structure

The crystal structure of the complex of the KB5-C20 TCR scFv [Vα2.3(AV2S3)-JαA10/Vβ2(BV2S1)-Dβ2-Jβ2.3] and Désiré-1 Fab has been determined to 2.6 Å resolution (see Materials and methods and Table I). The model is well defined except for the extra eight amino acids unique to the N-terminus of Vα2 polypeptides (Gahéry-Ségard *et al.*, 1996; Grégoire *et al.*, 1996) and the 24 residue linker used to connect the Vα and Vβ domains (Grégoire *et al.*, 1996). All these residues were omitted from the final model. Structure solution and refinement statistics are given in Table II.

Figure 1 shows the backbone ribbon representation of the complex. All six Fab CDRs interact with the TCR scFv ($CDR1_L$, six residues; $CDR2_L$, one residue; $CDR3_L$, three residues; $CDR1_H$, three residues; $CDR2_H$, five residues; $CDR3_H$, five residues). The antibody-accessible surface area buried by the interaction with the TCR Fv is 1343 Å^2 as calculated with X-PLOR (Brünger, 1990) using a 1.5 Å radius probe. Conversely, the areas of the buried surfaces on the Vα and Vβ domains correspond to 545 Å^2 (22 residues) and 833 Å^2 (26 residues), respectively. Consistent with the anti-clonotypic nature of the Désiré-1 antibody, the segments of the KB5-C20 TCR scFv that interact with Désiré-1 encompass both Vα and Vβ CDRs. As shown in Figure 1, the Vα CDR3 interacts with Fab residues contributed by the $CDR2_L$, $CDR1_H$ and $CDR3_H$, whereas the Vβ CDR2 interacts with $CDR3_L$ and $CDR2_H$ residues. It should be emphasized that the only contact between the Vβ CDR3 and the Désiré-1 Fab is the perpendicular interaction of the aromatic rings of W100β and Y32$CDR1_L$. The limited number of TCR CDRs involved in the interaction with the Désiré-1 Fab fragment is reflected by the fact that the geometrical centre of the Fab–TCR interface lies near the c′ strand of the TCR Vβ domain. This is in contrast with the structure of an Fab–anti-idiotype Fab complex (Bentley *et al.*, 1990) where

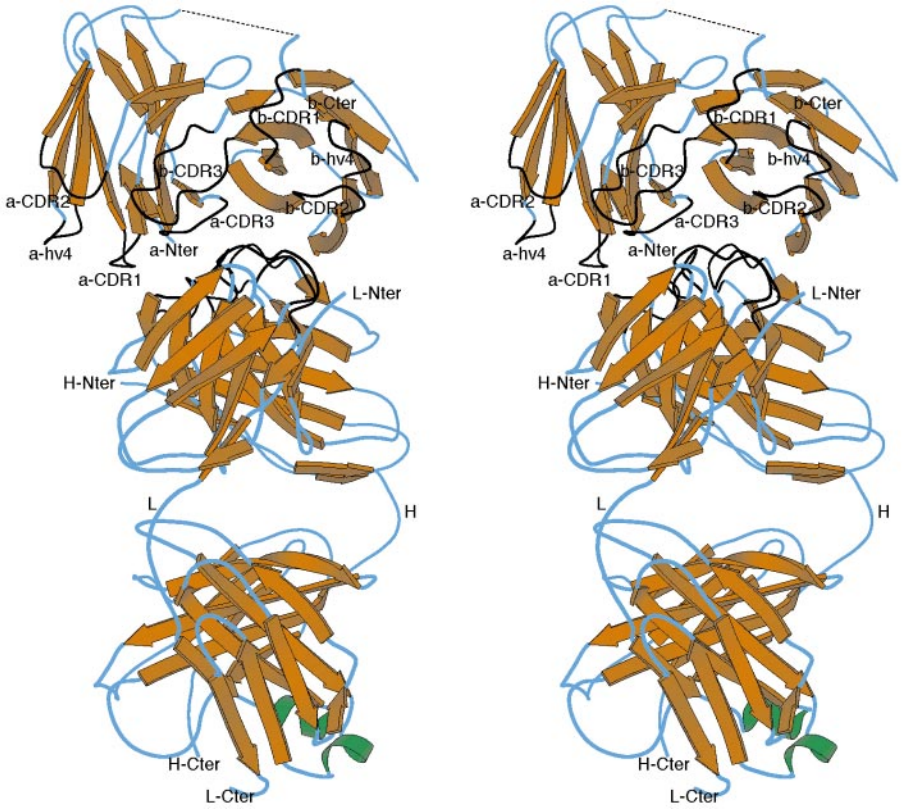

Fig. 1. Overall stereoscopic view of the complex between the KB5-C20 TCR scFv and Désiré-1 Fab fragment. The TCR scFv is at the top of the figure. The β strands were determined with the program PROCHECK (Laskowski *et al.*, 1993), and are represented as arrows, the α helices are depicted in green, and the CDRs as black coils.The β strands are labelled according to Bork *et al.* (1994). The linker connecting the C-terminus of Vα to the N-terminus of Vβ is not seen in the electron density map and is depicted as a dotted line. Its path appears to influence neither the Vα–Vβ association, nor the CDR conformation. This figure was produced with MOLSCRIPT (Kraulis, 1991). Abbreviations are as follows: a, TCR Vα domain; b, TCR Vβ domain; H, Ig heavy chain; L, Ig light chain; N-ter, NH_2-terminus; C-ter, COOH-terminus.

the two Ig Fab fragments are roughly aligned along their longest dimension and interact mostly through their respective CDRs. Therefore, bacterial superantigens (Fields *et al.*, 1996), peptide–MHC complexes (Garboczi *et al.*, 1996) and the Désiré-1 antibody (this paper) differ markedly in the way they bind to TCR V domains. Nevertheless, these TCR ligands are all capable of efficiently activating T cells.

The topology of Vα and Vβ domains

The amino acid sequence of the Vα2.3 segment used by the KB5-C20 TCR is 26% identical to that of the Vα4.2 segment used by the 1934.4 TCR (Fields *et al.*, 1995). Despite their identical names, note that the Vα2.3 segment used by the KB5-C20 TCR does not constitute the mouse homologue of the Vα2.3 segment found in the human A6 TCR (Clark *et al.*, 1995; Garboczi *et al.*, 1996). Accordingly, these two Vα segments share only 48% identity at the protein level. Based on the analysis of the three-dimensional structures of the 1934.4 Vα4.2 and 2C Vα3 segments, TCR Vα domains have been shown to be unique among Ig-related V domains in that their fifth β-strand (also known as c″; Bork *et al.*, 1994) forms hydrogen bonds with the d strand of the outer β-sheet (Fields *et al.*, 1995; Garcia *et al.*, 1996a). Such a switch of the c″ strand from the inner to the outer β-sheet was found to remove a surface protrusion from the Vα domain and, based on the packing found in a Vα crystal (Fields *et al.*, 1995), was hypothesized to permit the initiation of T-cell activation via αβ TCR dimerization (Fields *et al.*, 1995). In the KB5-C20 Vα domain, the c″ strand is also switched (Figure 2A). Moreover, consistent with their relative levels of primary sequence identities, the KB5-C20 Vα2.3 polypeptide backbone superposes better with A6 Vα2.3 than with Vα4.2 [root mean square (r.m.s.) differences of 0.77 and 0.92 Å are obtained for the positions of 98 pairs and 86 pairs of structurally equivalent α carbons, respectively; Figure 2A].

The amino acid sequence of the Vβ2 segment used by the KB5-C20 TCR is 27% identical to that of the Vβ8.2 domain used by both the 14.3.d and 2C TCRs (Bentley *et al.*, 1995; Garcia *et al.*, 1996a), and 28% identical to the human Vβ12.3 segment used by the A6 TCR (Garboczi *et al.*, 1996). When the KB5-C20 Vβ domain is superimposed onto its 14.3.d and A6 counterparts, r.m.s. differences of 0.98 and 1.04 Å are obtained for 78 and 80 pairs of equivalent α carbons, respectively. The major differences are restricted to the CDR3 region and c″ strand. As shown in Figure 2B, the four residue long c″ strand found in the KB5-C20 Vβ domain is hydrogen-bonded to the d strand of the outer β-sheet. This folding topology is different from those of the Vβ8.2 and Vβ12.3 domains

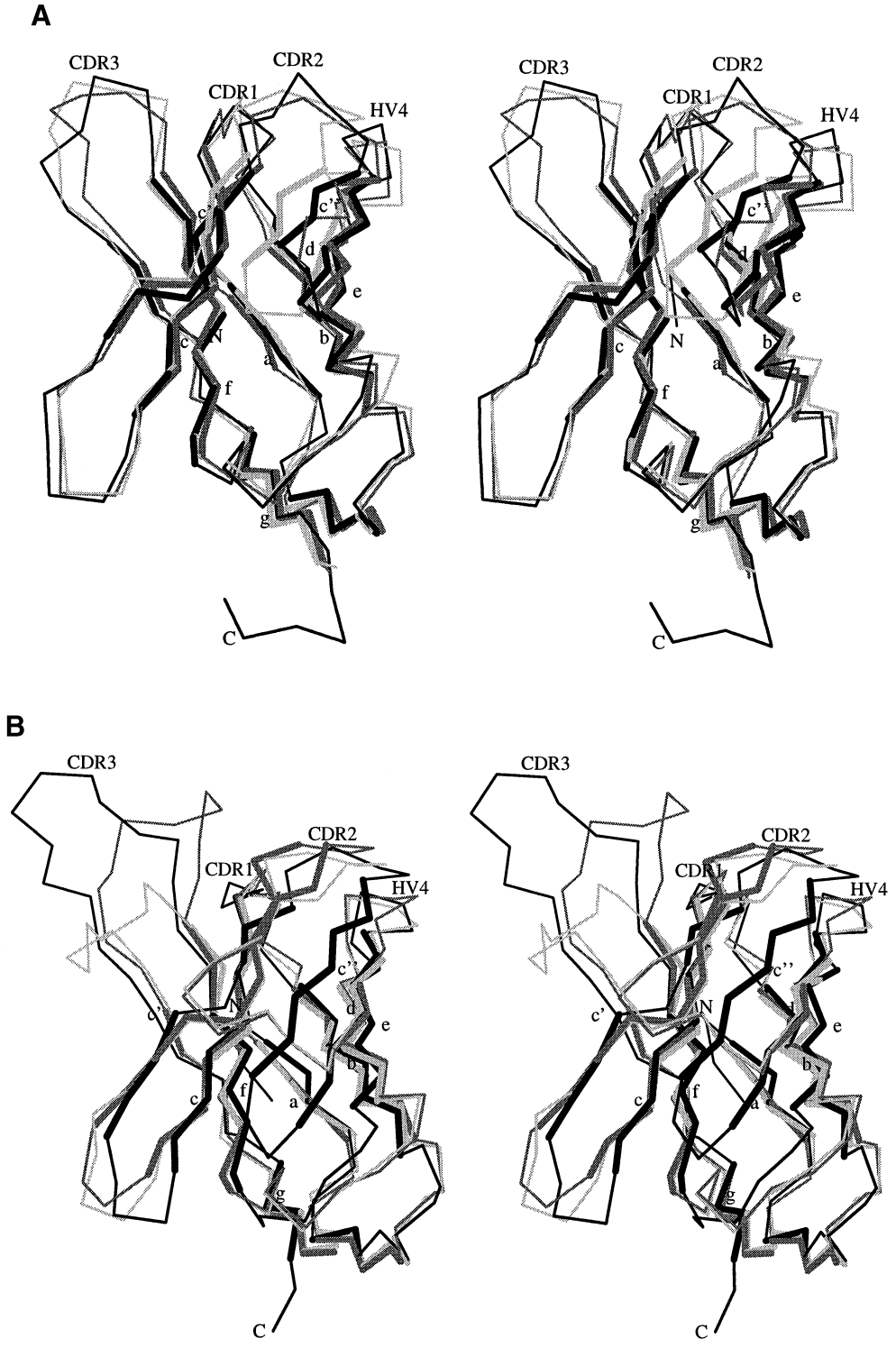

Fig. 2. Stereoscopic view of the α-carbon backbone of TCR Vα and Vβ domains. V domains were optimally superimposed with the program ALIGN (Satow *et al.*, 1986). The β strands are represented as thick lines and labelled according to Bork *et al.* (1994). (**A**) Diagram of the KB5-C20 Vα2.3 domain (black) superposed onto the A6 Vα2.3 (dark grey) and 1934.4 Vα4.2 (light grey) domains. Note that the CDR loops found in the KB5-C20 Vα2.3, 1934.4 Vα4.2 and A6 Vα2.3 domains display closely related conformations. (**B**) Diagram of the KB5-C20 Vβ2 domain (black) superposed onto the A6 Vβ12.3 (dark grey) and 14.3.d Vβ8.2 (light grey) domains. The c″ strand of the KB5-C20 Vβ domain is switched and hydrogen bonded to strand d, as previously observed in the A6 Vα2.3, 2C Vα3, 1934.4 Vα4.2 and KB5-C20 Vα2.3 domains. In the KB5-C20 Vβ2 domain, both the c″ and d strands are three residues longer than those found in the 14.3.d Vβ8.2 domain (see Table III). The 14.3.d CDR3β is three residues shorter than the KB5-C20 CDR3β, and adopts a different conformation, presumably due to the lack of Vα partner in the 14.3.d Vβ structure. The A6 CDR3β is two residues shorter than the KB5-C20 CDR3β and its tip folds away from CDR3α, opening a cavity at the CDR3α–CDR3β interface that accommodates the side chains of the central residues of the HTLV-1 peptide (Garboczi *et al.*, 1996).

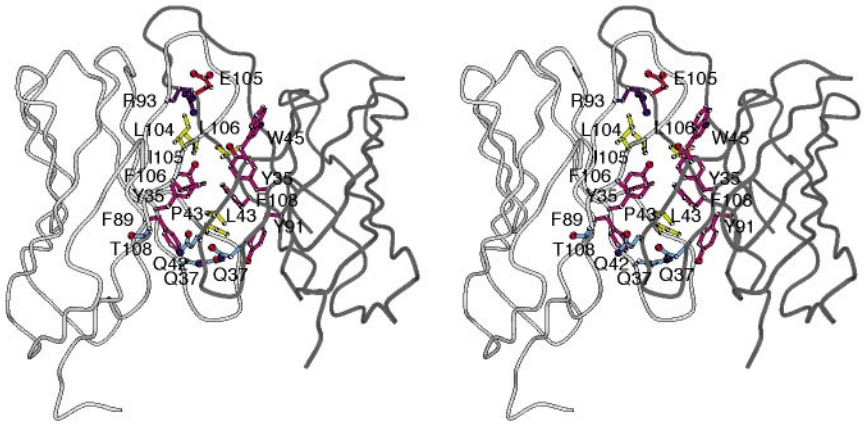

Fig. 3. Stereoscopic view of the KB5-C20 Vα–Vβ interface. The Vα and Vβ domains are on the left and right sides, respectively. Only side chains of residues involved in interdomain interactions are shown. Residues are colour-coded according to their chemical nature. Acidic residues are red, basic residues dark blue, polar residues light blue, hydrophobic residues yellow and aromatic residues purple.

(Table III, Bentley *et al.*, 1995; Garboczi *et al.*, 1996; Garcia *et al.*, 1996a), and reminiscent of the ones observed for the strand-switched Vα domains found in the 1934.4, 2C, A6 and KB5-C20 TCRs (Fields *et al.*, 1995; Garboczi *et al.*, 1996; Garcia *et al.*, 1996a; this paper). Therefore, the switch of strand c″ from the inner to the outer β-sheet does not constitute an exclusive attribute of TCR Vα domains. Inspection of the crystal structure of the KB5-C20 TCR scFv (this paper), and of available full-length TCR β chain structures (Bentley *et al.*, 1995; Garboczi *et al.*, 1996), further indicates that the switch of the c″ strand observed in the KB5-C20 Vβ2 domain results neither from artefactual contacts with the Désiré-1 Fab fragment, nor from the absence of the TCR Cβ domain [in the structures solved by Bentley *et al.* (1995) and Garboczi *et al.* (1996), the Cβ domain does not contact this part of the Vβ domain].

The Vα–Vβ interface

In the KB5-C20 TCR scFv, the Vα and Vβ domains are related by a 175° rotation axis. The accessible surface areas buried at the Vα–Vβ interface are 1029 Å^2 for Vα and 1067 Å^2 for Vβ. Thus, a total surface area of 2096 Å^2 is buried at the KB5-C20 interface, as opposed to values of 1160 and 1575 Å^2 in the cases of the 2C and A6 Vα–Vβ interfaces, respectively (Garboczi *et al.*, 1996; Garcia *et al.*, 1996a). Such scattered values are mostly accounted for by the differential contribution of residues belonging to CDRs (mainly CDR3s), which is higher in the KB5-C20 and A6 TCRs than in the 2C TCR. Many of the contacts between the KB5-C20 Vα and Vβ domains are conserved in the 2C and A6 TCRs, as well as in Ig V domains (Chothia *et al.*, 1985; Garboczi *et al.*, 1996; Garcia *et al.*, 1996a). Figure 3 shows the Vα–Vβ contacts found in the KB5–C20 TCR scFv. They include a pair of side chain–side chain hydrogen bonds between Q37α and Q37β, a symmetric pair of side chain–main chain hydrogen bonds involving Y35α–L106β and L104α–Y35β, and a hydrophobic core formed by Y35α, P43α, F89α, F106α, Y35β, L43β, L106β and F108β. Other interdomain contacts occur between residues I105α and W45β, as well as between the main chain oxygen of F106α and Q42β.

Table III. List of the β-sheet hydrogen bonds found between the c″–d and c′–c″ strands in the KB5-C20 Vα domain and in the KB5-C20, 14.3.d and A6 Vβ domains

KB5-C20 Vα2.3		KB5-C20 Vβ2		14.3.d Vβ8.2 and A6 hVβ12.3	
c″	d	c″	d	c′	c″
54O	N66	54O	N69		
56N	O64	56N	O67	48O	N56
56O	N64	56O	N67	48N	O56
58N	O62	58N	O65	46O	N58
58O	N62	58O	N65		
		60N	O63		
		60O	N63		

As discussed below, in the absence of peptide–MHC ligand, the KB5-C20 Vα and Vβ CDR3s protrude from the plane formed by the remaining CDRs and show a rather extensive contact surface area. A major feature of this CDR3α–CDR3β interface is the presence of an ionic interaction between R93α and E105β (Figure 3). Additional stabilization of this composite protrusion comes from several van der Waals contacts and two hydrogen bonds (Q95αN$^{\varepsilon 2}$–W100βO and G69αN–S103βO$^{\gamma}$). Composed of 13 residues, the KB5-C20 CDR3β loop contrasts with the shorter CDR3β loops found in the 2C and A6 Vβ domains (Figure 4), and interacts with CDR1α through a hydrogen bond between N30α and G101β. On the other hand, the KB5-C20 CDR3α loop interacts with CDR2β through a hydrogen bond between the main chain oxygen of R101α and the side chain of T48β. Comparison of our data with those reported by Garcia *et al.* (1996a) and Garboczi *et al.* (1996) indicates that the KB5-C20, 2C and A6 TCRs adopt very similar interdomain β-sheet packings, and suggests that neither the binding of the Désiré-1 Fab nor the absence of TCR C domains have significantly modified the native association of the V domains present in the KB5-C20 TCR scFv. Considering that some of the V segments used by these three TCRs share <30% amino acid sequence identity, our data further suggest that the identical mode of packing observed in these three TCRs is likely to constitute a general model

Clone	CDR1 α	CDR2 α	CDR3 α: Vα	N	Jα	CDR3 length
	24 32	48 56	88		109	
KB5-C20 (Vα2.3-JαA10)	Y E D S T F N Y F	S I R S V S D K K	Y F C A A	R	Y Q G G R A L I F G T G	8
2C (Vα3-Jα58)	Y S Y S A T P Y L	K Y Y S G D P V V Q	Y F C A V S		G F A S A L T F G S G	7
1934.4 (Vα4.2-Jα40)	Y S A S G Y P A L	R A S R D K E K G	Y Y C A L	S E	N Y G N E K I T F G A G	9
A6 (hVα2.3-Jα24)	Y S D R G S Q S F	S I Y S N G D - K	Y L C A V		T T D S W G K L Q F G A G	8

Clone	CDR1 β	CDR2 β	CDR3 β: Vβ	N / Dβ / N	Jβ	
	25 32	48 56	90		111	
KB5-C20 (Vβ2-Dβ2–Jβ2.3)	L K N S Q Y P W M	T L R S P G D K E	L Y C T C S A	A P D W G A	S A E T L Y F G S G	13
2C (Vβ8.2-Dβ2–Jβ2.4)	Q T N N H N - N M	Y S Y G A G S T E	Y F C A S G	G G G	T L Y F G A G	6
14.3.d (Vβ8.2-Jβ2.1)	Q T N N H N - N M	Y S Y G A G S T E	Y F C A S G	G G R G S	Y A E Q F F G P G	10
A6 (hVβ12.3-Dβ2-Jβ2.7)	Q D M N H E - Y M	Y S V G A G I T D	Y F C A S	R P G L A G G R P	E Q Y F G P G	11

Fig. 4. Comparison of primary sequences of the KB5-C20 Vα and Vβ complementarity-determining regions (CDR1, 2 and 3) with those found in Vα and Vβ domains of known three-dimensional structure. Note that the CDR3s found in the KB5-C20 and 2C TCR β chains differ both in their length and glycine residue content. The KB5-C20 CDR3β contains proline, tryptophan and aspartic acid residues which are contributed by N or D nucleotides and appear to be selected for in the CDR3β harboured by $CD8^+$ cells (Candéias *et al.*, 1991). The CDR boundaries are as defined in Chothia *et al.* (1988). Pannetier *et al.* (1993) have organized mouse Vβ segments into six groups sharing amino acid sequence homologies within their CDR1 regions. The Vβ2 segment used by the KB5-C20 TCR is characteristic of a group having CDR1s composed of nine amino acids (instead of eight amino acids as in most other Vβs), and containing Gln at position 29. Residues are numbered according to Kabat *et al.* (1991). In the case of the KB5-C20 Vβ domain, the primary sequence alignment deduced from the three-dimensional structures differs slightly from the one based on the comparison of primary sequences (Kabat *et al.*, 1991), and it is Cys92β (and not Cys94β) that forms the highly conserved disulfide bridge with Cys23β. Gaps are represented as dashes. Sequences are shown in the single-letter amino acid code and referenced in the text.

for the association of TCR Vα and Vβ domains. A similar conclusion has been drawn by Garboczi *et al.* (1996) when comparing the 2C and A6 TCRs.

TCR CDR loop conformations

In the case of Igs, five of the six CDRs that form the antibody-binding sites are known to adopt a small repertoire of main chain conformations stabilized by interactions between a few conserved residues belonging to the CDRs themselves and to the β-sheet framework buried beneath them (Chothia *et al.*, 1989). We have aligned the primary sequences of the KB5-C20, 2C, A6, 1934.4 and 14.3.d TCR V domains to determine the extent to which their CDR primary structures are similar (Figure 4). As previously observed for the Vα3 and Vα4.2 CDR1s, the conformation of the KB5-C20 CDR1α and CDR1β loops appears to be stabilized predominantly by hydrophobic interactions involving residues F29α and P30Aβ, respectively [these two residues are structurally equivalent to P30 of Vα3 (Garcia *et al.*, 1996a) and Vα4.2 (Fields *et al.*, 1995)]. This mode of stabilization contrasts with the intraloop hydrogen bonding observed in the case of the Vβ8.2 CDR1 (Bentley *et al.*, 1995). The KB5-C20 CDR1β and CDR2β are stabilized through additional interactions with residue R69β of the d–e loop [a loop also known as the fourth hypervariable region (HV4); Jores *et al.*, 1990)]. As shown in Figure 2B, in the absence of peptide–MHC ligand, the tip of CDR3β is stabilized by a hydrogen bond between the main chain NH group of W100 and the side chain of S103. The CDR2α of KB5-C20 is very similar to the corresponding region of A6 except for the insertion of residue V52, a protruding residue that may be implicated in peptide–MHC recognition (Figure 2A). As shown in Figure 2A, the KB5-C20 and 1934.4 CDR2αs are more dissimilar. The predominant interaction in the KB5-C20 CDR2α takes place between

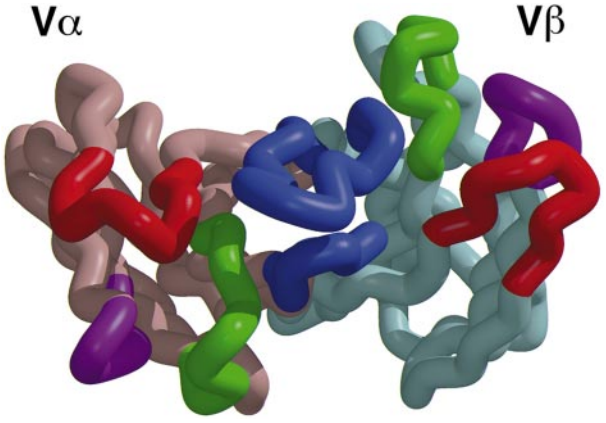

Fig. 5. Depiction of the α-carbon backbone of the KB5-C20 Vα and Vβ domains. The following colour codes have been used: Vα in light brown, Vβ in light blue, CDR1s in green, CDR2s in red, CDR3s in blue and HV4s in violet. In this orientation, the antigen-binding site is viewed from above, as in Figure 7B in Garcia *et al.* (1996a).

I49α and four other hydrophobic residues (F32α, I64α, F66α and L73α). Lys68 is conserved in the KB5-C20, 1934.4 and A6 Vαs, where it forms hydrogen bonds with neighbouring CDR1α residues. Finally, the KB5-C20 CDR3α forms two main chain–main chain hydrogen bonds with CDR1α and is stabilized by an intraloop hydrogen bond involving R93α and the main chain oxygen of G97α.

Structural comparison of Vα2 subfamily members

The Vα2.3 used by the KB5-C20 TCR belongs to a subfamily of Vα gene segments composed of 10 members which display >80% identity in their amino acid sequences (Gahéry-Ségard *et al.*, 1996). Comparison of their sequences shows the presence of conservative and non-conservative replacements within the CDRs (CDR1, positions 26, 28, 30; CDR2, positions 48, 50, 51, 54), as well

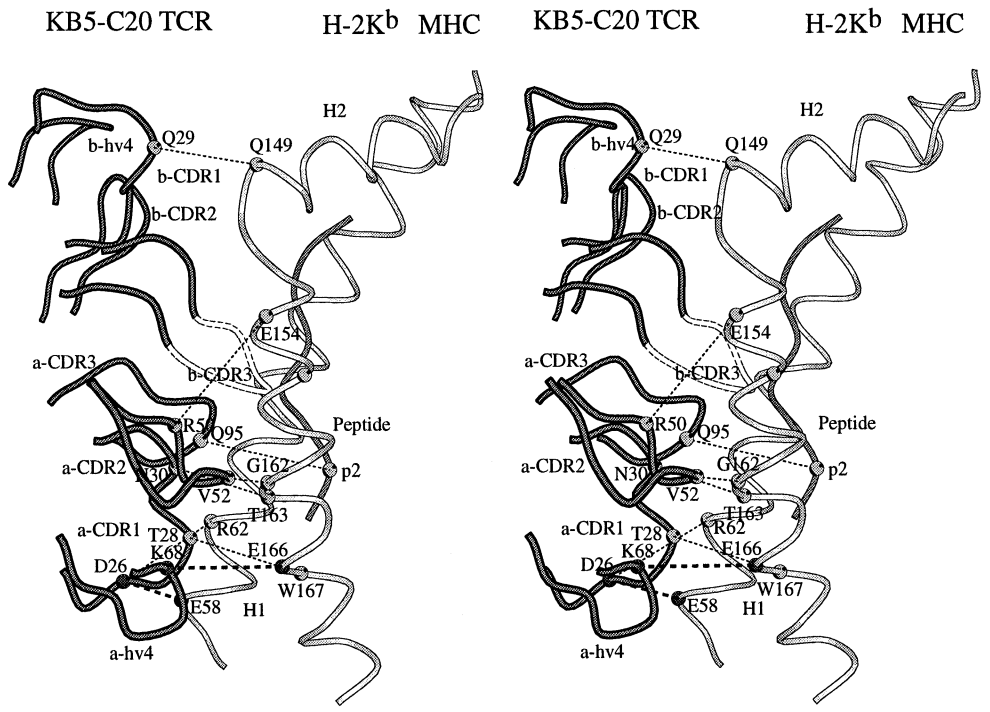

Fig. 6. Stereo pairs depicting plausible contacts between the KB5-C20 TCR CDR loops (dark grey), a bound octapeptide (medium grey) and the H-2K^b α1 and α2 helices (light grey). In this orientation, the TCR–peptide–MHC complex is viewed from the side, so that the H-2K^b α2 helix is in the foreground and the α1 helix is behind the peptide. The interactions between the KB5-C20 TCR and its cognate peptide–MHC complex were modelled by rotating these molecules onto the positions occupied by their human counterparts found in the A6 TCR–Tax–HLA-A2 complex (Garboczi *et al.*, 1996). These plausible interactions are depicted as dashed lines connecting the corresponding pairs of α-carbons. The interactions also present in the A6 TCR–Tax–HLA-A2 complex are shown as bold dashed lines, whereas those specific to the KB5-C20 TCR–peptide–H-2K^b complex are depicted as thin dashed lines. The configuration adopted by the peptide–MHC-unliganded CDR3β is shown as a dashed loop. Note that the interaction of residue Q95α with the second carbonyl group of the bound octapeptide is topologically equivalent to the one observed between residue Q30α of the A6 TCR and the second carbonyl function of the Tax nonapeptide. The superposition of the α1α2 domains of H-2K^b (PDB accession No. 1VAC) and HLA-A2 gives r.m.s. deviation of 0.66 Å. Abbreviations: a, TCR Vα chain; b, TCR Vβ chain; p2, position 2 of the octapeptide bound in the groove of the H-2K^b molecule.

as in the framework (positions 7, 16, 18, 19, 21, 36, 40, 42, 64, 72, 73, 78). Based on the three-dimensional structure of the Vα2.3 segment reported here, most of the residues varying within the mouse Vα2 subfamily could be assigned to lateral, solvent-exposed regions, and the few which are buried (positions 18, 36, 42, 64, 73), or located at the Vα–Vβ interface (position 48), should not modify the overall three-dimensional structure. Thus, the pattern of Vα folding is likely to be closely conserved within a given Vα subfamily.

The TCR antigen-binding site

As shown in Figure 5, the six CDRs cluster together at the membrane-distal tip of the KB5-C20 TCR scFv, the α and β HV4 loops lying at opposite ends of the binding site. Visual inspection of the recently published structure of the 2C TCR combining site (Garcia *et al.*, 1996a) and rigid-body rotation of the KB5-C20 TCR scFv onto the A6 TCR structure reported by Garboczi *et al.* (1996) indicate that the relative positions of the CDRs, with the exception of CDR3β, are rather conserved in these three TCR antigen-binding sites (compare Figures 2 and 5 with Figure 7B in Garcia *et al.*, 1996a). However, as expected from the fact that their respective CDR3β sequences lie at three scattered points of the size distribution observed for TCR β chain CDR3s (Candéias *et al.*, 1991; Pannetier *et al.*, 1993), the major differences between the structures of these TCR binding sites are confined to the CDR3β loops. As shown in Figure 5, the elongated KB5-C20 CDR3β loop packs tightly against the CDR3α loop without leaving an intervening hydrophobic pocket as found in both the A6 and 2C TCR binding sites (Garboczi *et al.*, 1996; Garcia *et al.*, 1996a). Moreover, in the absence of peptide–MHC ligand, the KB5-C20 CDR3α and CDR3β protrude from a plane formed by the remaining CDRs, thereby occupying a central position in the binding site.

A most remarkable feature of the structure of the KB5-C20 TCR combining site is the presence of a tryptophan residue (W100β) at the tip of CDR3β (Figure 7B). A few other large side chains are also present at the apex of the KB5-C20 CDRs (R50α, R69α, Q95α, Y30β, R50β). Solvent-exposed aromatic residues frequently have been observed in the CDRs of antibody-binding sites (reviewed in Padlan, 1994; Davis and Cohen, 1996), as well as in the binding site of the growth hormone receptor, where they occupy the centre of the contact interface and contribute to virtually all the binding energy (Wells, 1996). When considered together, the above features significantly differentiate the peptide–MHC-unliganded KB5-C20 TCR binding site from those of the unliganded 2C and liganded A6 TCRs, both of which present relatively flat surfaces (Garboczi *et al.*, 1996; Garcia *et al.*, 1996a). Moreover, the comparison of the three-dimensional models of KB5-C20, A6 and 2C TCRs and the isolated Vα 1934.4 and Vβ 14.3.d domains mostly confirms the prediction that the CDR1 and CDR2 loops are less structurally diverse than the CDR3 loops (Figures 2 and 5).

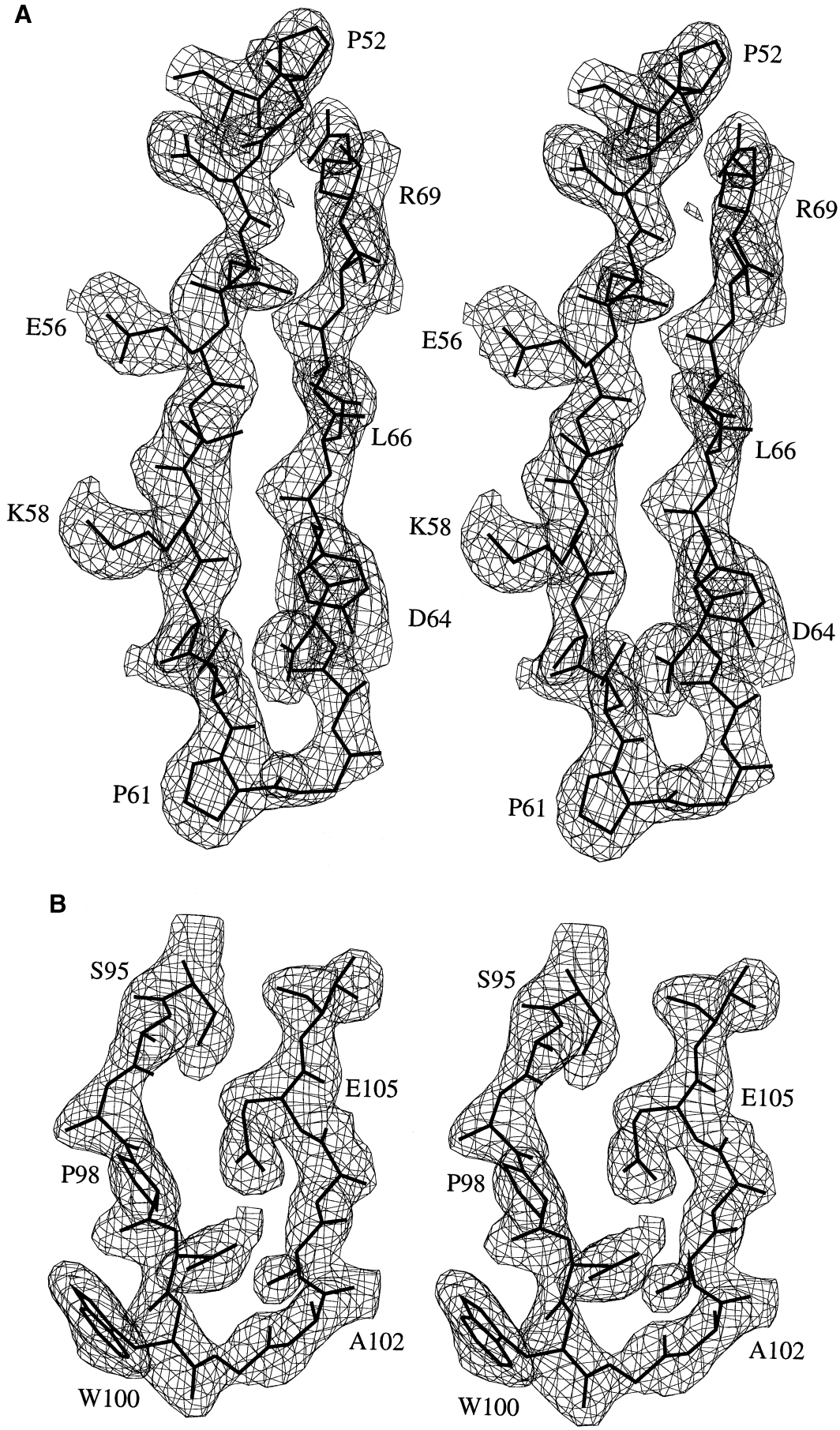
A
P52
R69
E56
L66
K58
D64
P61
P52
R69
E56
L66
K58
D64
P61
B
S95
E105
P98
A102
W100
S95
E105
P98
A102
W100

How does the KB5-C20 TCR see its ligand?

The approximate orientation of the 2C TCR docked to a peptide–H-2K^b complex has been determined using a set of X-ray data collected at 3.4 Å resolution (Garcia *et al.*, 1996a). A higher resolution picture of a TCR–peptide–MHC complex has been reported more recently by Garboczi *et al.* (1996). In the latter complex, the TCR is orientated diagonally across the peptide-binding site of HLA-A2, with the TCR Vα straddling the left end of the peptide-binding groove, so that CDR1α covers the amino-terminal part of the MHC α1 helix and CDR2α covers the carboxy-terminal part of the MHC α2 helix. In that orientation, the CDR3α and CDR3β loops contact the central region of the bound peptide and additionally interact with the MHC α1 and α2 helices, whereas CDR1α and CDR1β each contribute a single peptide-binding residue. Interestingly, the positioning of the Vα CDR1 and CDR2 over a zone of the peptide-binding groove, which distinguishes MHC class I and class II molecules (Brown *et al.*, 1993), provides a structural framework for recent functional data indicating that polymorphism in the CDR1 and CDR2 loops of Vα segments plays a salient role in distinguishing class I and class II MHC molecules (Sim *et al.*, 1996). In contrast to theoretical models (Davis and Bjorkman, 1988; Claverie *et al.*, 1989), in which all six TCR CDRs were hypothesized to interact simultaneously with the peptide–MHC complex, in the A6 TCR–Tax–HLA-A2 complex both CDR1β and CDR2β loops approach the carboxy-terminal end of the MHC α1 helix without contacting it. Moreover, contrary to these models, the TCR binding site solved by Garboczi *et al.* (1996) is not divided into two split binding surfaces, made of the CDR3s and of the remaining CDRs, and devoted to the independent recognition of the peptide and of the MHC, respectively. The diagonal orientation observed by Garboczi *et al.* (1996) for the A6 TCR–Tax–HLA-A2 complex may indeed constitute a general binding mode between TCR and MHC, in that it allows the flat surface of the TCR to interact maximally with the peptide, by fitting down between the two highest points on the MHC peptide-binding groove (see also Sun *et al.*, 1995). Considering that over half of the peptide surface is covered by CDR3β residues (Garboczi *et al.*, 1996), it should be noted that the short, glycine-rich, CDR3β loop which characterizes the 2C TCR binding site (Figure 4) is likely to account for its capacity to accommodate distinct peptide–MHC complexes (Tallquist *et al.*, 1996). Conversely, owing to their longer CDR3β loops, the KB5-C20 and A6 TCRs may have less flexibility in contacting the MHC-bound peptides and consequently display markedly increased peptide specificity relative to the peptide-promiscuous 2C TCR (Gavin and Bevan, 1995; Gilfillan *et al.*, 1995). Moreover, the long CDR3βs found in the KB5-C20 and A6 TCRs may act as a wedge and contribute to lift the Vβ CDR1 and CDR2 over the MHC peptide-binding groove.

Rigid-body rotations of the KB5-C20 TCR (this study) and H-2K^b (Fremont *et al.*, 1992; Zhang *et al.*, 1992) structures onto the A6 TCR–Tax–HLA-A2 complex reported by Garboczi *et al.* (1996) have allowed us to build a model from which plausible interactions between the KB5-C20 TCR and its cognate peptide–MHC ligand have been deduced. In the resulting hypothetical model shown in Figure 6, CDR2β and HV4β make no direct contact with the MHC molecule, whereas the CDR1β establishes only one interaction with H-2K^b (Q29β–Q149K^b). As a consequence, the surface of the H-2K^b peptide-binding groove is only partially engaged by the KB5-C20 TCR. Without resorting to translations along the peptide-binding site or rotations from the orientation observed by Garboczi *et al.* (1996), the inspection of the modelled complex using computer graphics revealed the existence of several plausible interactions involving three salt bridges (D26α–R62K^b, R50α–E154K^b and K68α–E166K^b), three hydrogen bonds (T28α–W167K^b, N30α–T163K^b, Q95α–main chain oxygen of peptide position P2) and one unambiguous van der Waals contact (V52α–G162K^b). Two of these interactions are conserved in the A6 TCR–Tax–HLA-A2 complex, whereas the remaining ones would be specific to the KB5-C20 TCR–peptide–H-2K^b complex (Figure 6).

The model shown in Figure 6 further indicates that the configuration of the KB5-C20 CDR3β loop found in the peptide–MHC unliganded TCR scFv structure is incompatible with ternary complex formation. To avoid colliding with the cognate peptide–MHC complex, a conformational change of the tip of the KB5-C20 CDR3β loop is required. By analogy with the configuration adopted by the CDR3β loop found in the A6 TCR–Tax–HLA-A2 complex (Garboczi *et al.*, 1996; see also Figure 2B), we suggest that, when complexed to its cognate peptide–MHC ligand, the tip of the KB5-C20 CDR3β loop adopts a different conformation removed from CDR3α (i.e. points upwards relative to the plane of Figure 6), so that it can interact with the C-terminal region of the bound peptide. No information is available yet on the primary sequence of the K^b-bound peptide(s) recognized by the KB5-C20 TCR (Guimezanes *et al.*, 1992). Its identification should allow us to determine crystallographically whether the KB5-C20 TCR recognizes peptide–K^b complexes with an orientation similar to the one observed for the A6 TCR–Tax–HLA-2 complex, implying a concurrent conformational change of its CDR3β loop. Finally, our data also bear on the role of the CD8 molecule during TCR recognition. It has been demonstrated recently that CD8 enhances the half-life of the interaction between a TCR and a peptide–MHC complex (Luescher *et al.*, 1995; Garcia *et al.*, 1996b). In addition to this well-documented off-rate decreasing function, CD8 may also help some TCRs, such as the one expressed by the KB5-C20 T cell, to adopt configurations that allow their proper interaction with the surface of the peptide–MHC ligand. For instance, once trapped closely together via CD8, the TCR may undergo multiple docking trials on the peptide–MHC ligand. Thus, by favouring 'lengthy collisions', CD8 may increase the probability of producing the correct complementarity of the interacting surfaces between some TCR CDRs and their corresponding peptide–MHC ligands.

Fig. 7. Stereo pairs of the electron density map of the model contoured at the σ level, and generated from SIGMAA-weighted $2mF_o–DF_c$ coefficients (Read, 1986). (**A**) The switched c″ strand and the d strand of the Vβ domain are shown to illustrate their extended interactions. (**B**) The CDR3β loop is very well defined in the electron density map.

Materials and methods

Protein expression and purification

KB5-C20 is an alloreactive mouse cytotoxic T-cell clone specific for H-2K^b molecules complexed with a peptide of unknown primary structure (Albert *et al.*, 1982). A recombinant KB5-C20 TCR scFv was produced in myeloma cells and purified as described previously (Grégoire *et al.*, 1996). N-terminal sequencing of the KB5-C20 TCR scFv gave a unique amino acid sequence (QQQEKRDQQVRQSQSLTVW in the one-letter code for amino-acids). A preparation yielding a single peak by ion-exchange chromatography was obtained by treatment of the native protein with neuraminidase. The neuraminidase-treated KB5-C20 TCR scFv is soluble and binds to all conformation-specific monoclonal antibodies available (Grégoire *et al.*, 1996). The monoclonal anti-clonotypic antibody Désiré-1 specific for the native KB5-C20 TCR (Grégoire *et al.*, 1991; Hua *et al.*, 1985) was cleaved by papain to yield an Fab fragment. The resulting Fab was purified further to homogeneity by successive runs on protein A–Sepharose and ion-exchange columns. Désiré-1, a mouse IgG2a, expresses a H chain made of a V_H gene segment of the J558 family, a D_H gene segment not assignable to any known group and a J_H2 gene segment. Its L chain is composed of a V_κ gene segment strongly homologous to the V_κ gene segment K2 (Nishioka and Leder, 1980) and of a $J_\kappa2$ gene segment.

Protein crystallization and data collection

Two crystal forms of the neuraminidase-treated KB5-C20 TCR scFv complexed to the Fab fragment of the monoclonal anti-clonotypic antibody Désiré-1 (TCR scFv–Fab complex) were obtained from pre-incubated solutions containing a 1:1.5 TCR scFv:Fab ratio by using the hanging drop method (Wlodawer and Hodgson, 1975). The final crystallization conditions were 15% PEG6000, 100 mM HEPES buffer, pH 6.9–7.5, 200 mM NaCl and 0.1% NaN_3. X-ray diffraction data for the first crystal form were collected at –150°C at the European Synchrotron Radiation Facility (ESRF), beam line D14, using a CCD area detector. Images were corrected for spatial distortion with the program FIT2D (Hammersley *et al.*, 1994). Indexing and integration of the diffraction data were carried out using the program MOSFILM (Leslie, 1991). Data reduction and scaling were performed with SCALA and AGROVATA (CCP4, 1979). These procedures indicated that the crystals belong to the orthorhombic space group $P2_12_12$ with a = 184.3 Å, b = 80.4 Å and c = 104.2 Å. A maximum resolution of 2.9 Å was obtained under these conditions. V_m calculations, 5.0 Å^3/D for one complex in the asymmetric unit (Matthews, 1968), indicated the likely presence of two TCR scFv–Fab complexes per asymmetric unit. Data collection statistics are shown in Table I. Subsequently, data were collected for a second crystal form present in the crystallization drops (space group $P2_12_12$ with a = 187.3 Å, b = 81.0 Å and c = 52.1 Å, with one molecule per asymmetric unit). These experiments were carried out at the D2AM beam line of the ESRF, at cryogenic temperatures to a resolution of 2.5 Å. Data were processed using a modified version of XDS (Kabsch, 1988, 1993).

Structure solution

Since related three-dimensional structures were available for both the TCR and the Fab components of the complex, the molecular replacement program AMoRe (Navaza, 1994) was used for the structure solution. Data from the first crystal form between 15 and 3.5 Å were used throughout. A search for amino acid sequence homologies with the Désiré-1 Fab fragment in the Protein Data Bank (Berstein *et al.*, 1977, program BLAST, Altschul *et al.*, 1990) indicated that the best models were the corresponding domains of 1VFA (Bhat *et al.*, 1994) for V_L, 1MLB (Braden *et al.*, 1994) for V_H and 1FLR (Whitlow *et al.*, 1995) for both C_κ and C_H1. Because of the flexibility of the elbow angle connecting Ig variable and constant domains and the uncertainty concerning the TCR orientation, the molecular replacement procedure was carried out using three independent search bodies. The first body, consisting of the C_κ and C_H1 domains, gave two equivalent fairly well-contrasted solutions (see Table II); a similar result was obtained when using the V_L–V_H dimer as a one-body search model. From these searches, it was concluded that the two TCR scFv–Fab complexes in the asymmetric unit were related by an approximate half-unit cell translation in the *c*-axis direction. Subsequent combination of both variable and constant domains solutions resulted in a much improved correlation (Table II), indicating that the two whole Fab fragments had been placed correctly. Since the relative orientations of the Vα and Vβ domains of the TCR were not known, a VαVβ model based on the Vα homodimer structure (Fields *et al.*, 1995) was used to generate rotation function solutions. These solutions subsequently were tested in translation searches, after having fixed the Fab position in the asymmetric unit. Significant improvement in the correlation coefficient and *R*-factor indicated that this approach was correct. Previous attempts to use the individual TCR domains (either Vα or Vβ) in the rotation search systematically yielded only one of the two possible solutions, namely the one corresponding to the Vα domain. After applying the rigid-body refinement option of AMoRe, the *R*-factor for data between 10.0 and 3.0 Å resolution was 0.48. A few cycles of rigid-body refinement were sufficient to place correctly the structure of the refined model from the first crystal form in the second crystal form, and the corresponding *R*-factor was 0.41 for data between 10.0 and 3.0 Å.

Model building and refinement

The resulting rigid-body refined TCR scFv–Fab model was inspected in a SIGMAA-weighted (Read, 1986) electron density map using the graphics program O (Jones *et al.*, 1991). Most of the Fab regions were very well defined in the electron density, including the elbow segment that was not part of the search model. As expected from the amino acid sequence comparisons, major disagreements between the search model and the electron density were restricted to the TCR VαVβ domains. At this point, the model was corrected in those areas where modifications were immediately obvious. Other, more difficult parts were dealt with by temporarily setting their atomic occupancies to zero. A simulated annealing procedure using the program X-PLOR (Brünger, 1990) was then carried out. After several cycles of crystallographic refinement [using either X-PLOR or refmac (CCP4, 1979)] and model rebuilding using computer graphics, a much improved model was obtained. The following regions are still missing from the model: the N-terminal eight residues of Vα and the linker 24 residues. The *R*-factor for data with $F > 3\sigma(F)$ between 8 and 2.9 Å was 0.249 (see Table II).

Refinement of the second crystal form allowed for a significant improvement of the model (Table I). The approximate half-unit cell translation in the *c*-axis direction observed in the first crystal form is now an exact crystallographic operation. The current *R*-factor is 0.210 for data with a $F > 3\sigma(F)$ cut-off. The final electron density map is of good quality (Figure 7). All figures were generated using this second crystal form. The atomic coordinates have been deposited with the Protein Data Bank (accession code 1kb5).

Acknowledgements

We thank Anne-Marie Schmitt-Verhulst, Annick Guimezanes, Jean Davoust, Ginette Boulot, Lee Leserman and Pierre Golstein for discussions and comments on the manuscript, Anne-Marie Schmitt-Verhulst for originally providing the KB5-C20 T-cell clone and Désiré monoclonal antibody, P.Ghosh and D.C.Wiley for making the A6-TCR–Tax–HLA-2A complex coordinates available to us prior to release by the Protein Data Bank, Roy Mariuzza for providing the coordinates for 1934.4 Vα, Christine Gaboriaud and Pierre Legrand for their advice in the use of O, FIT2D and BLAST, Andy Thompson of Beam Line D14 from the European Synchrotron Radiation Facility, Grenoble, France, Jean-Luc Ferrer and Michel Roth from the French CRG D2AM beamline at ESRF and Noelle Guglietta for typing the manuscript. This work was supported by institutional grants from CNRS, CEA, INSERM and by specific grants from Ministère de l'Education Nationale et de la Recherche, Association pour la Recherche sur le Cancer and Ligue nationale Contre le Cancer.

References

Albert,F., Buferne,M., Boyer,C. and Schmitt-Verhulst,A.-M. (1982) Interactions between MHC-encoded products and cloned T-cells. I. Fine specificity of induction of proliferation and lysis. *Immunogenetics*, **16**, 533–549.

Altschul,S.F., Gish,W., Miller,W., Myers,E.W. and Lipman,D.J. (1990) Basic local alignment search tool. *J. Mol. Biol.*, **215**, 403–410.

Bentley,G.A., Boulot,G., Riottot,M.M. and Poljak,R.J. (1990) Three-dimensional structure of an idiotope–anti–idiotope complex. *Nature*, **348**, 254–257.

Bentley,G.A., Boulot,G., Karjalainen,K. and Mariuzza,R.A. (1995) Crystal structure of the β chain of a T cell antigen receptor. *Science*, **267**, 1984–1987.

Bernstein,F.C., Koetzle,T.F., Williams,G.J., Meyer,E.F.,Jr, Brice,M.D., Rodgers,J.R., Kennard,O., Shimanouchi,T. and Tasumi,M. (1977) The Protein Data Bank. A computer-based archival file for macromolecular structures. *Eur. J. Biochem.*, **80**, 319–324.

Bhat,T.N. *et al*. (1994) Bound water molecules and conformational stabilization help mediate an antigen–antibody association. *Proc. Natl Acad. Sci. USA*, **91**, 1089–1093.

Bork,P., Holm,L. and Sander,C. (1994) The immunoglobulin fold. Structural classification, sequence patterns and common core. *J. Mol. Biol.*, **242**, 309–320.

Braden,B.C., Souchon,H., Eisele,J.L., Bentley,G.A., Bhat,T.N., Navaza,J. and Poljak,R.J. (1994) Three-dimensional structures of the free and the antigen-complexed Fab from monoclonal anti-lysozyme antibody D44.1. *J. Mol. Biol.*, **243**, 767–781.

Brown,J.H., Jardetzky,T.S., Gorga,J.C., Stern,L.J., Urban,R.G., Strominger,J.L. and Wiley,D.C. (1993) Three-dimensional structure of the human class II histocompatibility antigen HLA-DR1. *Nature*, **364**, 33–39.

Brünger,A.T. (1990) *X-PLOR Manual (version 3.1).* Yale University, New Haven, CT.

Candéias,S., Waltzinger,C., Benoist,C. and Mathis,D. (1991) The Vβ17+ T cell repertoire: skewed Jβ usage after thymic selection; dissimilar CDR3s in $CD4^+$ versus $CD8^+$ cells. *J. Exp. Med.*, **174**, 989–1000.

CCP4 (1979) *The SERC Collaborative Computing Project No 4: A Suite of Programs for Protein Crystallography.* Daresbury Laboratory, Warrington WA4 4AD, UK.

Chothia,C., Novotny,J., Bruccoleri,R. and Karplus,M. (1985) Domain association in immunoglobulin molecules. The packing of variable domains. *J. Mol. Biol.*, **186**, 651–663.

Chothia,C., Boswell,D.R. and Lesk,M.A. (1988) The outline structure of the T-cell αβ receptor. *EMBO J.*, **7**, 3745–3755.

Chothia,C. *et al*. (1989) Conformations of immunoglobulin hypervariable regions. *Nature*, **342**, 877–883.

Clark,S.P., Arden,B., Kabelitz,D. and Mak,T.W. (1995) Comparison of human and mouse T-cell receptor variable gene segments families. *Immunogenetics*, **42**, 531–540.

Claverie,J.-M., Prochnika-Chalufour,A. and Bougueleret,L. (1989) Implications for a Fab-like structure for the T-cell receptor. *Immunol. Today*, **10**, 10–14.

Davies,D.R. and Cohen,G.H. (1996) Interactions of protein antigens with antibodies. *Proc. Natl Acad. Sci. USA*, **93**, 7–12.

Davis,M.M. and Bjorkman,P.J. (1988) T-cell antigen receptor genes and T-cell recognition. *Nature*, **334**, 395–401.

Fields,B.A. *et al*. (1995) Crystal structure of the Vα domain of a T cell antigen receptor. *Science*, **270**, 1821–1824.

Fields,B.A., Malchiodi,E.M., Li,H., Ysern,X., Stauffacher,C.V., Schlievert,P.M., Karjalainen,K. and Mariuzza,R.A. (1996) Crystal structure of a T-cell receptor β-chain complexed with a superantigen. *Nature*, **384**, 188–192.

Fremont,D.H., Matsumura,M., Stura,E.A., Peterson,P.A. and Wilson,I.A. (1992) Crystal structures of two viral peptides in complex with murine MHC class I $H\text{-}2K^b$. *Science*, **257**, 919–927.

Fremont,D.H., Stura,E.A., Matsumura,M., Peterson,P.A. and Wilson,I.A. (1995) Crystal structure of an $H\text{-}2K^b$–ovalbumin peptide complex reveals the interplay of primary and secondary anchor positions in the major histocompatibility complex binding groove. *Proc. Natl Acad. Sci. USA*, **92**, 2479–2483.

Gahéry-Ségard,H., Jouvin-Marche,E., Six,A., Gris-Liebe,C., Malissen,M., Malissen,B., Cazenave,P.-A. and Marche,P.N. (1996) Germline genomic structure of the B10.A mouse Tcra-V2 gene subfamily. *Immunogenetics*, **44**, 298–305.

Garboczi,D.N., Ghosh,P., Utz,U., Fan,Q.R., Biddison,W.E. and Wiley,D. (1996) Structure of the complex between human T-cell receptor, viral peptide and HLA-A2. *Nature*, **384**, 134–141.

Garcia,K.C., Degano,M., Stanfield,R.L., Brunmark,A., Jackson,M.R., Peterson,P.A., Teyton,L. and Wilson,I.A. (1996a) An αβ T cell receptor structure at 2.5 Å and its orientation in the TCR–MHC complex. *Science*, **274**, 209–219.

Garcia,K.C., Scott,C.A., Brunmark,A., Carbone,F.R., Peterson,P.A., Wilson,I.A. and Teyton,L. (1996b) CD8 enhances formation of stable T-cell receptor/MHC class I molecule complexes. *Nature*, **384**, 577–581.

Gavin,M.A. and Bevan,M.J. (1995) Increased peptide promiscuity provides a rationale for the lack of N regions in the neonatal T cell repertoire. *Immunity*, **3**, 793–800.

Gilfillan,S., Bachmann,M., Trembleau,S., Adorini,L., Kalinke,U., Zinkernagel,R., Benoist,C. and Mathis,D. (1995) Efficient immune responses in mice lacking N-region diversity. *Eur. J. Immunol.*, **25**, 3115–3122.

Grégoire,C., Rebao,N., Schweisguth,F., Necker,A., Mazza,G., Auphan,N., Millward,A., Schmitt-Verhulst,A.-M. and Malissen,B. (1991) Enginered secreted T-cell receptor αβ heterodimers. *Proc. Natl Acad. Sci. USA*, **88**, 8077–8081.

Grégoire,C., Malissen,B. and Mazza,G. (1996) Characterization of T cell receptor single-chain Fv fragments secreted by myeloma cells. *Eur. J. Immunol.*, **26**, 2410–2416.

Guimezanes,A., Schumacher,T.N.M., Ploegh,H.L. and Schmitt-Verhulst, A.-M. (1992) A viral peptide can mimic an endogeneous peptide for allorecognition of a major histocompatibility complex class I product. *Eur. J. Immunol.*, **22**, 1651–1654.

Hammersley,A.P., Svensson,S.O. and Thompson,A. (1994) Calibration and correction of spatial distortions in 2D detector systems. *Nucl. Instrum. Methods A*, **346**, 312–321.

Hua,C., Buferne,M. and Schmitt-Verhulst,A.-M. (1985) Lysis of hybridoma cells bearing anti-clonotypic surface immunoglobulin by clonotype-expressing alloreactive cytotoxic T cells. *Eur. J. Immunol.*, **15**, 1029–1032.

Hue,I., Trucy,J., McCoy,C., Couez,D., Malissen,B. and Malissen,M. (1990) A novel type of aberrant T cell receptor α-chain gene rearrangement. Implications for allelic exclusion and the V–J recombination process. *J. Immunol.*, **144**, 4410–4419.

Jones,T.A., Zou,J.-Y., Cowan,S.W. and Kjeldgaard,M. (1991) Improved methods for building protein models in electron density maps and the location of errors in these models. *Acta Crystallogr.*, **A47**, 110–119.

Jores,R., Alzari,P.M. and Meo,T. (1990) Resolution of hypervariable regions in T-cell receptor β chains by a modified Wu–Kabat index of amino acid diversity. *Proc. Natl Acad. Sci. USA*, **87**, 9138–9142.

Kabat,E.A., Wu,T.T., Reid-Miller,M., Perry,H.M. and Gottesman,K.S. (1991) *Sequences of Proteins of Immunological Interest*. National Institutes of Health, Bethesda, MD.

Kabsch,W. (1988) Evaluation of single crystal X-ray diffraction data from a position sensitive detector. *J. Appl. Crystallogr.*, **21**, 916–924.

Kabsch,W. (1993) Automatic processing of rotation diffraction data from crystals of initially unknown symmetry and cell constants. *J. Appl. Crystallogr.*, **26**, 795–800.

Kraulis,P.J. (1991) Molscript: a program to produce both detailed and schematic plots of protein structures. *J. Appl. Crystallogr.*, **24**, 946–950.

Laskowski,R.A., MacArthur,M.W., Moss,D.S. and Thornton,J.M. (1993) PROCHECK—a program to check the stereochemical quality of protein structures. *J. Appl. Crystallogr.*, **26**, 283–291.

Leslie,A.G.W. (1991) Molecular data processing. In Moras,D., Podjarny,A.D. and Thierry,J.C. (eds), *Crystallographic Computing.* Oxford University Press, pp. 50–61.

Luescher,I.F., Vivier,E., Layer,A., Mahiou,J., Godeau,F., Malissen,B. and Romero,P. (1996) CD8 modulation of T-cell antigen receptor–ligand interactions on living cytotoxic T lymphocytes. *Nature*, **373**, 353–356.

Madden,D.R., Garboczi,D.J. and Wiley,D.C. (1993) The antigenic identity of peptide–MHC complexes: a comparison of the conformations of five viral peptides presented by HLA-A2. *Cell*, **75**, 693–708.

Matthews,B.W. (1968) Solvent content of protein crystals. *J. Mol. Biol.*, **33**, 491–497.

Navaza,J. (1994) AMoRe: an automated package for molecular replacement. *Acta Crystallogr.*, **A50**, 157–163.

Nishioka,Y. and Leder,P. (1980) Organization and complete sequence of identical embryonic and plasmacytoma kappa V-region genes. *J. Biol. Chem.*, **255**, 3691–3694.

Padlan,E.A. (1994) Anatomy of the antibody molecule. *Mol. Immunol.*, **31**, 169–217.

Pannetier,C., Cochet,M., Darche,S., Casrouge,A., Zöller,M. and Kourilsky,P. (1993) The sizes of the CDR3 hypervariable regions of the murine T-cell receptor β chains vary as a function of the recombined germ-line segments. *Proc. Natl Acad. Sci. USA*, **90**, 4319–4323.

Read,R. (1986) Improved Fourier coefficients for maps using phases from partial structures with errors. *Acta Crystallogr.*, **A42**, 140–149.

Satow,Y., Cohen,G.H., Padlan,E.A. and Davies,D. (1986) Phosphocholine binding immunoglobulin Fab McPC603: an X-ray diffraction study at 2.7 Å. *J. Mol. Biol.*, **190**, 593–604.

Sim,B.-C., Zerva,L., Greene,M.I. and Gascoigne,N.R.J. (1996) Control of MHC restriction by TCR Vα CDR1 and CDR2. *Science*, **273**, 963–966.

Sun,R., Shepherd,S.E., Geier,S.S., Thomson,C.T., Sheil,J.M. and Nathenson,S.G. (1995) Evidence that the antigen receptors of cytotoxic T lymphocytes interact with a common recognition pattern on the H-2K^b molecule. *Immunity*, **3**, 573–582.

Tallquist,M., Yun,T.J. and Pease,L.R. (1996) A single T cell receptor recognizes structurally distinct MHC/peptide complexes with high specificity. *J. Exp. Med.*, **184**, 1017–1026.

Wells,J.A. (1996) Binding in the growth hormone receptor complex. *Proc. Natl Acad. Sci. USA*, **93**, 1–6.

Whitlow,M., Howard,A.J., Wood,J.F., Voss,E.W.,Jr and Hardman,K.D. (1995) 1.85 Angstroms structure of anti-fluorescein 4-4-20 Fab. *Protein Eng.*, **8**, 749–761.

Wlodawer,A. and Hodgson,K.O. (1975) Crystallisation and crystal data of monellin. *Proc. Natl Acad. Sci. USA*, **72**, 398–399.

Young,A.C., Zhang,W., Sacchettini,J.C. and Nathenson,S.G. (1994) The three-dimensional structure of H-2D^b at 2.4 Å resolution: implications for antigen-determinant selection. *Cell*, **76**, 39–50.

Zhang,W., Young,A.C.M., Imarai,M., Nathenson,S.G. and Sacchettini,J.C. (1992) Crystal structure of the major histocompatibility complex class I H-2K^b molecule containing a single viral peptide: implications for peptide MHC binding and T-cell receptor recognition. *Proc. Natl Acad. Sci. USA*, **89**, 8403–8407.

Received on February 19, 1997; revised on April 7, 1997